Measurement of $R = \sigma_L/\sigma_T$ on Deuterium in the Nucleon Resonance Region and Beyond: A proposal to PAC29

Nov 30, 2005

J. Arrington
Argonne National Laboratory, IL

I. Albayrak, M.E. Christy (spokesperson), C.E. Keppel (spokesperson), S. Malace, V. Tvaskis
Hampton University, Hampton, VA

E. Kinney
University of Colorado, Boulder, Colorado

P. Markowitz, J. Reinhold
Florida International University, University Park, FL

I. Niculescu, G. Niculescu
James Madison University, Harrisonburg, VA

J. Dunne
Mississippi State University, Mississippi State, MS

A. Gasparian
North Carolina A&T State University, Greensboro, NC

A. Bodek, R. Bradford, S. Manley, K. McFarland, J. Steinman
University of Rochester, Rochester, NY

P. Bosted, A. Bruell, R. Ent, D. Gaskell, M. Jones, D. Mack, S. Wood
Thomas Jefferson National Accelerator Facility, Newport News, VA

H. Gallager
Tufts University, Medford, MA

O. Rondon, K. Slifer
University of Virginia, Charllotsville, VA

H.P. Blok
Vrije Universiteit, Amsterdam, Netherlands

H. Mkrtchyan, R. Asaturyan, V. Tadevosyn
Yerevan Physics Institute, Yerevan, Armenia

Abstract

We propose to measure the longitudinal/transverse (L/T) separated structure functions from deuterium from the quasielastic region through the nucleon resonance region ($1 < W^2 < 4$ GeV^2) and beyond to $W^2 \approx 4.5$ GeV^2 and spanning the four-momentum transfer range $1 < Q^2 < 4.5$ (GeV/c)^2. The separation of the inclusive electroproduction cross sections into longitudinal and transverse strengths will be accomplished by performing Rosenbluth separations to extract the transverse structure function $F_1(x, Q^2)$, the longitudinal structure function $F_L(x, Q^2)$, $F_2(x, Q^2)$, and the ratio $R = \sigma_L \ / \ \sigma_T$. This proposal represents a critical continuation of the first global survey of these fundamental separated quantities on deuterium which began with the low Q^2 data taking period of E02-109 [1].

The excellent precision obtained from the measurement of the separated proton data in the resonance resonance region from E94-110 [2, 3] and in the DIS from E99-118 [4, 5], both of which were performed in Hall C, will be presented. The extension of the proton measurements to deuterium is straightforward and allows the precision of the proposed measurements to be predicted with great confidence. The great care and time invested in developing the experimental requirements, systematic uncertainty measurements, and analysis machinery will be of immediate benefit to the proposed experiment. This is confirmed by the excellent data quality obtained during the E02-109 run period, which will also be presented.

The separated L/T structure functions are fundamental properties of the nucleons. As such, the measurement of these *fundamental* quantities allows a variety of physics issues to be addressed, including: QCD moments of the deuterium and neutron structure functions, neutron elastic form factors, and quark-hadron duality in protons and neutrons.

Finally, the proposed measurements are necessary for meeting one of the stated DOE milestones for hadronic physics, which is to "Measure the lowest moments of the unpolarized nucleon structure functions (both longitudinal and transverse) to 4 GeV^2 for the proton and neutron ...". Experimentally determining both the proton and neutron moments provide a direct confrontation with recent and future calculations from lattice QCD of the nucleon non-singlet moments. The proposed measurements will allow a precision determination of the moments for the *complete* set of unpolarized structure functions of the deuteron and neutron in the range $0.5 < Q^2 < 4.5$ GeV^2. This extended Q^2 range is needed to separate higher twist components from the leading twist, which can then be compared directly to the recent lattice calculations performed at $Q^2 = 4$ GeV^2.

The proposed precision cross section measurements will be made in Hall C using the HMS spectrometer (to collect electron yields) and the SOS spectrometer (for background measurements) and utilizing standard 4 cm cryogenic deuterium and hydrogen targets. This is a base equipment experiment and requires little time for setup and checkout. To perform L/T separations we require different beam energies of 2.35, 3.49, 4.63, and 5.77 GeV at a base linac energy of $E_{base} = 1.14$ GeV and 4.05 GeV at $E_{base} = 0.8$ GeV. The total beam time requested to make these important measurements is 13 days.

1 Experiment Overview

We propose to measure the deuteron L/T separated structure functions in the nucleon resonance region for $0.5 < Q^2 < 4.5$ GeV^2. This requires precision measurements of the inclusive e-d cross section and can be accomplished utilizing only the base Hall C spectrometers and cryogenic target assembly. A significant portion of the data required to perform the separation of the unpolarized structure functions for $Q^2 < 2$ GeV^2 was

taken in January of 2005 as part of E02-109. E02-109 was approved by PAC22 to perform L/T separations on deuterium for $0.5 < Q^2 < 4$ GeV^2 and received only a portion of the approved beam time before entering jeopardy status. The subsequent jeopardy proposal submitted to PAC28 requesting the remaining beam time needed to both reduce the uncertainties for the low Q^2 and to extend the L/T separations up to $Q^2 = 4$ GeV^2 was deferred 'with regret'.

In this proposal we shall attempt to elucidate the critical role of these fundamental measurements in the endeavor to understand nucleon structure and, in particular, to fulfill Jefferson Lab's mandate to extend our understanding of the transition from perturbative to non-perturbative QCD. The high luminosity provided by the CEBAF electron beam at Jefferson Lab combined with the proven capability of the Hall C HMS spectrometer to make precision cross section measurements allows these measurements to be performed in a modest number of days, and provides a unique opportunity to perform the *definitive* measurements of the deuteron unpolarized structure functions in this kinematic region. We, therefore, request 13 days of beam to complete these important measurements.

2 Formalism

Due to the small value of the electromagnetic coupling constant, the scattering of electrons from nucleons can be well approximated by the exchange of a single virtual photon, which carries the exchanged 4-momentum squared, q^2. In terms of the incident electron energy, E, the scattered electron energy, $E^{'}$, and the scattering angle, θ, the absolute value of the exchanged 4-momentum squared is given by

$$-q^2 = Q^2 = 4EE^{'}\sin^2\frac{\theta}{2}. \tag{1}$$

In the one photon exchange approximation, the spin-independent cross section for inclusive electron-nucleon scattering can be expressed in terms of the photon helicity coupling as

$$\frac{d\sigma}{d\Omega dE^{'}} = \Gamma\left[\sigma_T(x,Q^2) + \epsilon\sigma_L(x,Q^2)\right], \tag{2}$$

where σ_T (σ_L) is the cross section for photo-absorption of purely transverse (longitudinal) polarized photons,

$$\Gamma = \frac{\alpha E^{'}(W^2 - M_p^2)}{2\pi Q^2 M_p E(1-\epsilon)} \tag{3}$$

is the flux of virtual photons, and

$$\epsilon = \left[1 + 2(1+\frac{\nu^2}{Q^2})\tan^2\frac{\theta}{2}\right]^{-1} \tag{4}$$

is the relative flux of longitudinal virtual photons.

In terms of the structure functions $F_1(x,Q^2)$ and $F_2(x,Q^2)$, the double differential cross section can be written as

$$\frac{d\sigma}{d\Omega dE'} = \Gamma \frac{4\pi^2\alpha}{x(W^2-M_p^2)} \left[2xF_1(x,Q^2) + \epsilon \left(\frac{1+4M_p^2x^2}{Q^2} F_2(x,Q^2) - 2xF_1(x,Q^2) \right) \right]. \tag{5}$$

Comparison of equations 2 and 5 shows that $F_1(x,Q^2)$ is purely transverse, while the combination

$$F_L(x,Q^2) = \frac{1+4M_p^2x^2}{Q^2} F_2(x,Q^2) - 2xF_1(x,Q^2) \tag{6}$$

is purely longitudinal. The separation of the unpolarized structure functions into longitudinal and transverse parts from cross section measurements can be accomplished via the Rosenbluth technique [6], by making measurements at two or more values of ϵ for fixed x and Q^2. Fitting the reduced cross section, $d\sigma/\Gamma$, linearly in ϵ, yields σ_T (and therefore $F_1(x,Q^2)$) as the intercept, and the structure function ratio $R(x,Q^2) = \sigma_L/\sigma_T = F_L(x,Q^2)/2xF_1(x,Q^2)$ as the slope. We note that $F_2 \propto 2xF_1 + F_L$ can only be extracted from cross sections either by measuring at $\epsilon = 1$ or by performing L/T separations. At typical JLab kinematics the contribution of F_L to F_2 can be significant.

3 Motivation and Goals

The measurements proposed here are fundamental. By definition, therefore, they will have bearing on a wide variety of physics topics and measurements. This section discusses these topics, and includes neutron and deuterium structure functions, structure function moments, non-singlet evolution, elastic form factors, spin dependent structure functions, and global modeling for neutrino oscillation experiments. The measurements here proposed are crucial to every one of these topics.

3.1 Existing Data

The existing World resonance region measurements of R on deuterium from SLAC [7, 8, 9] are shown in Figure 1 as a function of both W^2 and Q^2. In this region the data is both sparse and of low quality, with typical errors on R of 100% or larger. In addition, there are no deuterium measurements of R below $W^2 < 2.5$ GeV^2. This prevents any extraction of the separated structure functions from deuterium for the lower mass resonances. For the proton measurements, PAC 11 stated that "the L/T ratio on the proton is a fundamental quantity that should be measured with the best possible accuracy." This argument is no less true for the deuteron, the simplest nuclear system, or for the neutron. A comparison of the resonance region proton R values measured in the range $1.5 < Q^2 < 2.5$ GeV^2 by E94-110 (blue triangles) to the entire SLAC data set (red circles) for $Q^2 < 9$ GeV^2 is shown in Figure 2. The measurements proposed here will essentially duplicate the quality of the proton data on the deuteron. Neutron data will be obtained by subtracting the proton data from the proposed deuterium data, and after applying nuclear corrections. This will be discussed in more detail in Section 3.3.

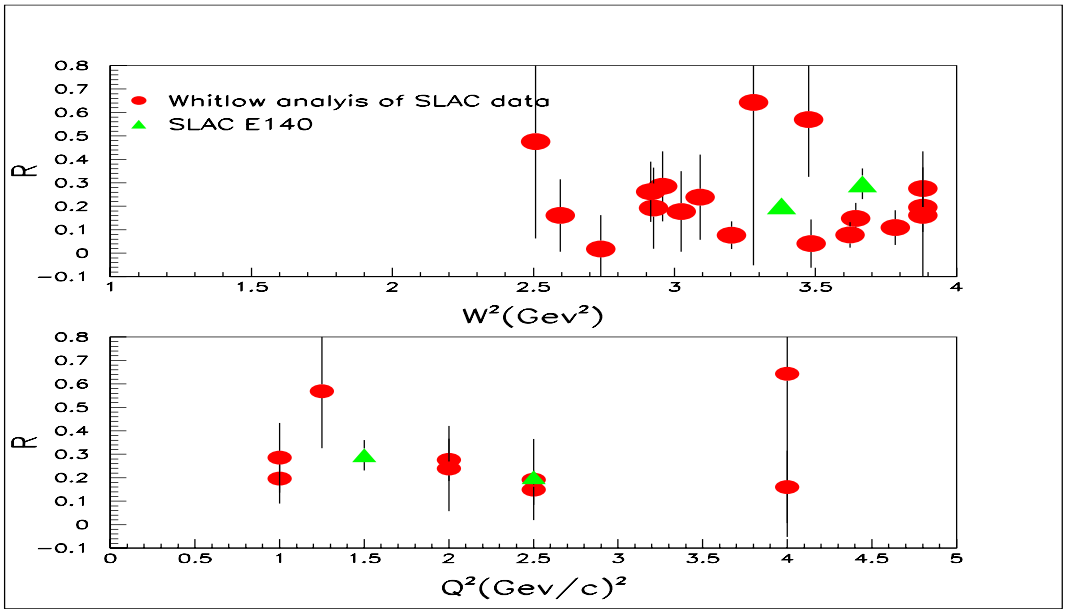

Figure 1: The world's data set of R on deuterium in the resonance region with W^2 (top) and Q^2 (bottom). The top panel includes measurements which extend to $Q^2 = 20$ (GeV/c)^2.

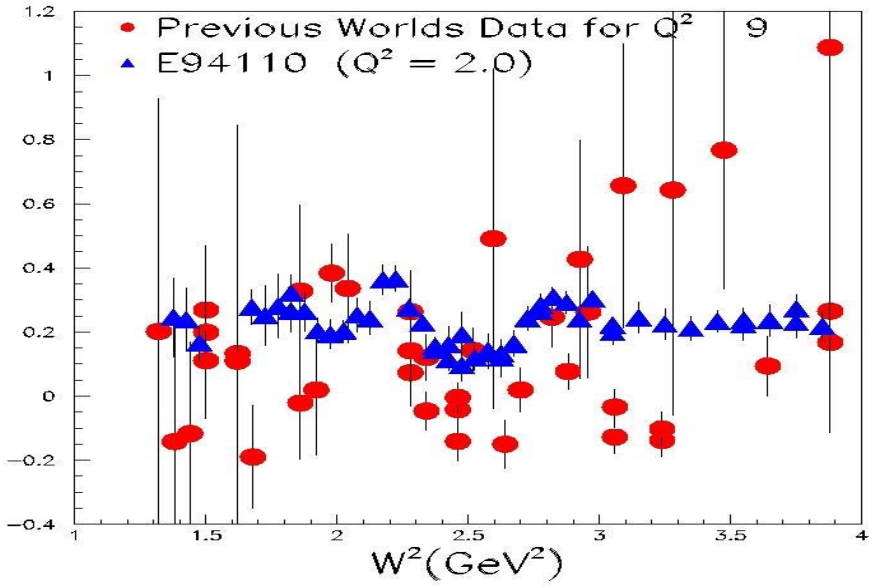

Figure 2: Resonance region measurements of proton R from E94-110 for $1.5 < Q^2 < 2.5$ GeV^2 (blue triangles) and the previous world data set (red circles) for $Q^2 < 9$ GeV^2 as a function of W^2.

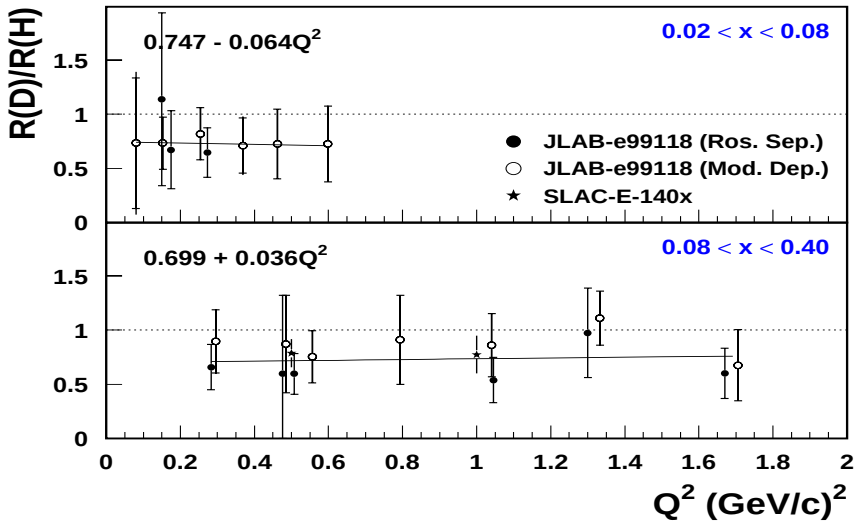

Figure 3: The ratio $\frac{R_d}{R_p}$ as measured by JLab E99-118 and SLAC E140 at low Q^2.

3.2 Is R_d Different from R_p?

It is often assumed that R_d is equal R_p, where R_p is R measured on the proton. This assumption is based on the previously available deep inelastic scattering data [8, 10], where it was found that the difference between R_d and R_p was small. This is not surprising since, at the typically higher Q^2 values of the available deep inelastic data, R itself is quite small. Additionally, these data have significant error bars and as such are marginally sensitive to differences in small R values. These deep inelastic data are shown in Figure 3, below, in comparison to preliminary results (taken from the thesis of V. Tvaskis [5]) obtained by the recent Hall C measurements [5] from Experiment E99-118 [4, 5]. This JLab experiment was approved, specifically, to investigate the low x and low Q^2 regime. Nonetheless, it provides a first hint that R_d may in fact *NOT* be equal to R_p in the region where R is not small. From the plot, one can see that R_d is surprisingly only 70% as large as R_p. This hints that the neutron longitudinal component is smaller than the proton, although a difference is also suggested by some nuclear models (see, for example, Reference [11]). The proposed experiment will be able to verify the E99-118 result, and extend the measurement to the larger x and larger Q^2 regime.

3.3 Neutron and Deuterium Structure Function Extractions

The sensitivity to R of the extraction of F_2 from cross section measurements is an important consideration for the Barely off-shell Neutron Structure (BoNuS) experiment [12], which is currently completing in Hall B during Fall/Winter 2005. BoNuS was designed to measure the inclusive cross section for electrons scattering from a gas deuterium target while tagging on a slow backward proton. The tagging of these slow

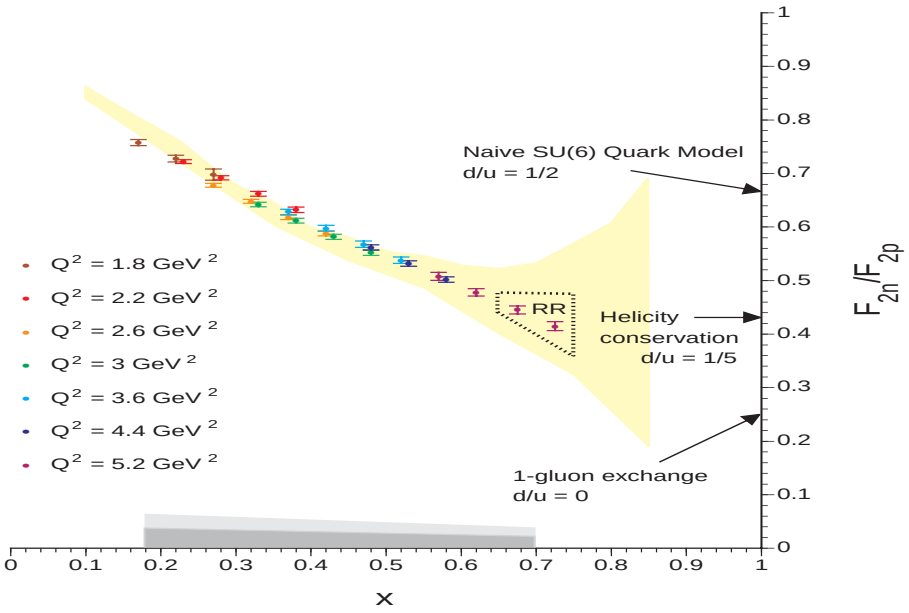

Figure 4: Estimated results for F_2^n/F_2^p from BoNuS for several Q^2 values. The points with (statistical) error bars are the expected BoNUS results (which have been slightly offset for each Q^2) and the dark shaded band at the bottom represents the total expected point-to-point uncertainty. The yellow banded area is the current estimated theoretical uncertainty on extracting this ratio utilizing inclusive deuteron and proton data.

recoil protons ensures that they are spectators and therefore, that the scattering was from a 'nearly' free neutron. A wide range of W^2 values from the quasielastic region to the DIS ($W^2 > 4$ GeV^2) are accessed by BoNuS. This will allow the ratio F_2^n/F_2^p to be determined with relatively small uncertainties at large x values, where previous determinations of this ratio using SLAC deuterium and proton data suffer from large uncertainties in the nuclear corrections (arising from Fermi motion, binding, and off-shell effects). The size of the nuclear uncertainties in the SLAC determinations are represented by the yellow band in Figure 4, while the quality of the expected BoNuS data is represented by the points with (statistical) error bars.

For the highest beam energy of $E = 5.25$ GeV utilized during the 2005 BoNuS run, the sensitivity of the F_2^n extraction on the assumed value for R is shown in Figure 5. Here the ratios of the F_2 values extracted using $R = 0.2$ to that using $R = 0$ are shown. The measurements proposed here are very complimentary to the free neutron cross section measurements of BoNuS. BoNuS was proposed to provide neutron cross sections with systematic uncertainties of $\approx 5\%$ [12], but will not provide any information on the separated cross sections. The proposed experiment, on the other hand, will provide L/T separated cross sections on deuterium. In addition, BoNuS will provide valuable information on the correct prescription for nuclear corrections which can then be applied to the separated deuterium cross sections.

The procedure would be to first separate the contributions from the longitudinal and transverse deuteron cross sections and then to apply the nuclear corrections to these separated cross sections. Conservatively assuming that these corrections can be

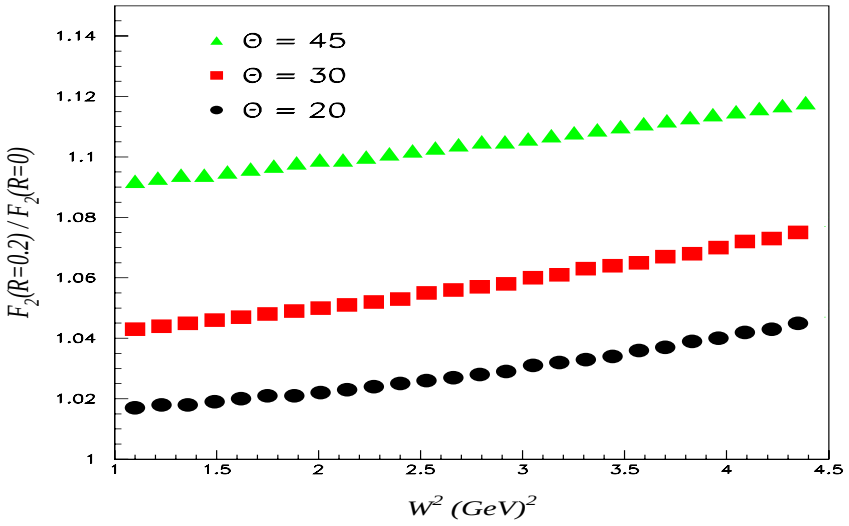

Figure 5: Sensitivity of the extraction of F_2 on the value of R for BoNuS resonance region kinematics at the highest beam energy of E = 5.25 GeV and scattering angles of θ = 20, 30, and 45°.

determined to even the 10% level utilizing the BoNuS data, the contribution of this additionally uncertainty would still allow a reasonably precise determination of F_1^n and F_L^n in the resonance region. This can be envisioned by examining the precision E94-110 proton structure functions in Figure 6 with an additional uncertainty of 10%. We further note that an examination of the E94-110 F_L data near the edge of the resonance region at W^2 =4 GeV^2 ($x = 0.49$ at $Q^2 = 3$) shows that the proton measurements significantly improve on the precision of the existing SLAC data at these kinematics, where most of the L/T separations were performed by combining cross section measurements from several experiments with different systematics. Extending the deuteron measurements from $W^2 = 4$ (the maximum for the proton measurements) to $W^2 = 4.5$ GeV^2 would allow the minimum x measured to move from 0.49 to 0.45, and would have a significant impact on the current precision of the deuteron F_L measurements in this range. Since the data at higher W^2 comes in faster, this only increases our beam time request by one additional day, but significantly enhances the determination of the moments, which are discussed in the next section.

3.4 Moments of Unpolarized Structure Functions for the Deuteron and Neutron

In the time since the original E02-109 proposal, developments in experiment and theory have served to enhance both the relevance and timeliness of the proposed measurements. On the experimental side is the running of the BoNuS experiment already discussed, while on the theoretical side is the calculation of the nucleon non-singlet QCD moments which have now been performed [13, 14, 15] on the lattice for $Q^2 = 4$ GeV^2. The proposed deuterium measurements combined with the corresponding proton measurements,

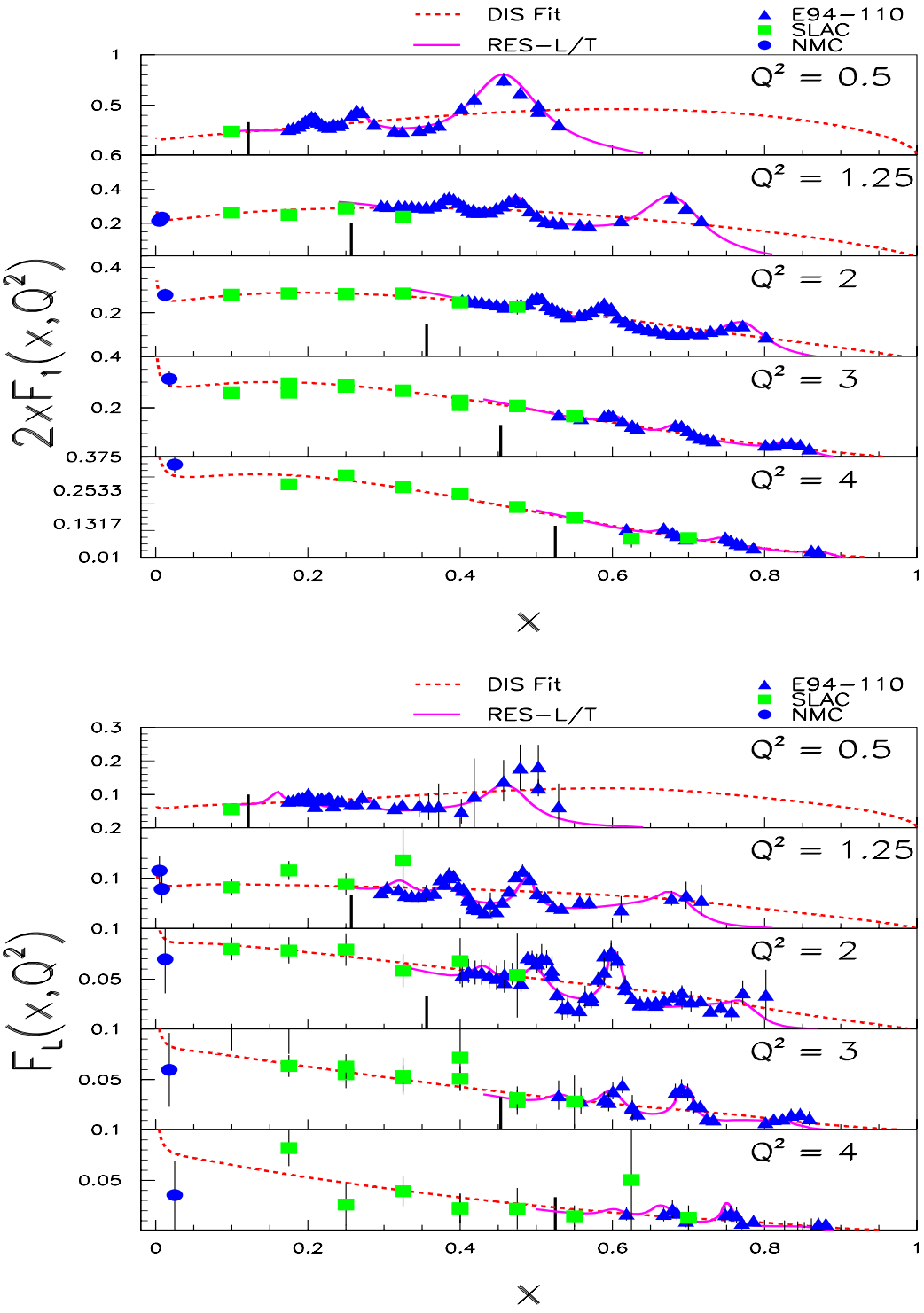

Figure 6: Rosenbluth extracted data for proton F_1 (top) and F_L (bottom). The triangles represent the E94-110 data with full statistical and systematic error bars included. The solid curve is the result of the global fitting procedure, while the dashed curve is a fit to DIS data. The vertical black line represents the value in x of $W^2 = 4.5$ GeV^2.

already performed in Hall C, will allow for a direct confrontation of these, and future, calculations with precision data.

The Cornwall-Norton moments of the structure functions are defined as

$$M_n^{2,L}(Q^2) \equiv \int_0^1 dx \;\; x^{n-2} \; F_{2,L}(x, Q^2) \tag{7}$$

and

$$M_n^1(Q^2) \equiv \int_0^1 dx \;\; x^{n-1} \; F_1(x, Q^2). \tag{8}$$

At $Q^2 = 4$ GeV^2 the proposed data are critical since the resonance region extends down to $x = 0.6$ and comprises a significant (and in the case of the higher moments, the dominant) contribution to the moments. This is easily observed from an examination of the proton results in Figure 6. These measurements will allow for a determination of the Q^2 evolution of these moments. This could play a crucial role in understanding the transition from perturbative to nonperturbative QCD in nucleon structure and, consequentially, is listed as one of the DOE's stated milestones for hadronic physics. For reference, the complete list of the DOE's hadronic physics milestones is given in Appendix A.

Without this proposed measurement, it will be impossible for Jefferson Lab to meet this milestone. The resonance region data are crucial to accurate moment extraction. The n-p moments are the least model-dependent non-singlet quantity to obtain. Deuterium data are crucial to the neutron moments and, even with the BONUS neutron cross sections, L/T separations will be required.

At small Q^2 the resonance region contribution to the moments can be significant, and even dominant for the higher moments. This is evident from Table 1, where the percentage contribution of the resonance region to the n=2 and n=4 moments of the longitudinal and transverse structure functions has been estimated utilizing the proton data for $Q^2 = 1.5$, 3, and 4 GeV^2. On the other hand, the uncertainty on the extracted n=2 neutron moments arising from the nuclear corrections has been estimated in Table 2, and is found to be only about 5-6% at $Q^2 = 4$ GeV^2. Utilizing the BoNuS data should allow this additional uncertainty to be eliminated almost entirely. The percentage uncertainties in the deuteron (neutron) F_L moments without these measurements is a significant fraction of the percentages given in Table 1, since F_L^d is not very well constrained by the the current resonance region data.

Q^2 (GeV^2)	F_1 (n=2)	F_1 (n=4)	F_L (n=2)	F_L (n=4)
1.5	55%	91%	48%	89%
3.0	24%	64%	21%	64%
4.0	15%	49%	13%	52%

Table 1: Percentage resonance region contribution to the transverse and longitudinal structure function moments, estimated from the proton data.

A precise determination of the non-singlet moments requires the best possible measurements of the proton and neutron structure functions across the entire x range. This

n	F_2	F_1	F_L
2	5.2%	5.2%	5.9%
4	12.1%	12.6%	16.8%

Table 2: Percentage contribution of the nuclear corrections to the uncertainty on the extraction of the neutron moments from the proposed measurements, at $Q^2 = 4$ GeV^2. Estimates were made based on the E94-110 proton data.

is because the non-singlet moments can only be determined from *differences* of proton and neutron moments. Using the estimated uncertainties on F_2^d due to the current uncertainties on R_d at typical JLab kinematics, we estimate the current uncertainty due to R_d on the $n = 2$ moment of F_2^{ns} (F_2 non-singlet) to be $\approx 9\%$ at $Q^2 = 4$ GeV^2 (with the uncertainty on the $n = 4$ moment being significantly larger). The corresponding uncertainties at smaller Q^2 values are significantly larger for F_2. The uncertainties F_1^{ns} are similar, while the uncertainties on F_L^{ns} are estimated at over 100% due to the current uncertainties on R_d. These uncertainties can not be reduced with the BoNuS data and to do so requires the proposed data.

3.5 Non-Singlet Evolution

This section was taken verbatim from a letter written in support of this proposal by Johannes Bluemlein of DESY.

The precise knowledge of the proton's flavor structure and the precision tests on the evolution of leading twist parton densities as predicted by QCD are key questions of present day studies of deeply inelastic scattering. On the first glance one may be curious about the fact that deuteron data should play any role in understanding the proton data. The flavor decomposition first requires, however,

i) separation between the flavor non-singlet and singlet evolution
ii) precision knowledge of u_v and d_v in the whole x-range - if possible at the same accuracy.

Down quarks can be measured best off neutrons, i.e. deuterons in praxi. To measure the non-singlet distributions in the whole x-range one needs

$$2F_2^p - F_2^d. \tag{9}$$

This is actually the only way in the non-valance region $x < 0.3$. In the valence region the information about d_v also comes from F_2^d in the first place due to the electromagnetic coupling. The deuteron wave function corrections are either well understood or under currently more detailed consideration, depending on the kinematic region.

An ideal running strategy consist in measuring:

$$F_2^p,\ F_L^p,\ F_2^d \text{ and } F_L^d$$

at sufficiently high statistics (if possible: equal statistics shall be reached). Having precision measurements for all these four functions available allows an unambiguous

approach to derive the respective flavor non-singlet distributions and the study of the singlet distributions due to the stronger gluon effects in F_L^i together with the F_2^i.

In particular, the JLAB data are unique. Not only, that the above data sets can be taken in the way as described: the statistics is also going to become sufficiently large to allow for precision measurements if the deuteron running is continued as planned by the collaboration. The combination of these measurements with the World DIS data at higher W^2 can lead to a very detailed picture of the physics behind the unpolarized JLAB DIS data:

i) twist-2 QCD contributions (determined widely model-independent)
ii) *experimental* extraction of the higher twist contributions in F_2^p, F_2^d, F_L^p, F_L^d in a single experiment with well-controlled systematics and very good statistics - this may allow for the first time a detailed measurement of these quantities as a function of x and in a *few* Q^2 bins - a world novelty
iii) These measurements can be compared with upcoming lattice simulations and perturbative QCD calculations to be performed.

Experiment would deliver here the first fundamental information in this field. These measurements would form a new, very non-trivial testing ground for QCD both in its non-perturbative and perturbative aspects.

In summary, highly precise deuteron data - due to the above aspects - are forming a conditio sine qua non for any real precision test of QCD.

3.6 Neutron Elastic Form Factors

The proposed measurements include the quasielastic region which is needed to separate quasielastic contributions from the low W^2 inelastic cross sections. While the quasielastic region is not the primary focus of this proposal, the data proposed will have statistics on par with the precision measurements [16] from SLAC experiment NE11, which extracted the electromagnetic neutron elastic form factors via Rosenbluth separations at Q^2 =1.75, 2.50, 3.25, and 4 GeV^2. In additon, while the ϵ arm will be similar to the NE11 measurements, the number of ϵ points at each Q^2 will be slightly larger and with reduced systematics on the cross sections since, in contrast to NE11, a single spectrometer will be used for the measurements at all ϵ values. Due to these combined effects, the proposed data would result in an overall reduction in the uncertainty of extracted electric (G_E^n) and magnetic (G_M^n) form factors of the neutron for $2 < Q^2 < 4$, where extractions using polarization observables do not currently exist.

3.7 Quark-Hadron Duality

The E94-110 proton R measurements allowed for the first precision tests of parton-hadron duality (for a recent overview see Reference [17]) in all unpolarized structure functions. With this and the previous JLab Hall C measurements, duality has been shown to be a fundamental property of proton structure. This work has inspired renewed interest in the topic from both an experimental and theoretical perspective (see for example [18, 19, 20, 21, 22]), and the proposed data will add valuable information. Specifically, Close and Isgur [23] argue that the neutron structure functions should exhibit "systematic deviations from local duality." In their approach, minimal necessary

conditions are identified for duality to occur in a simple harmonic oscillator quark model and these conditions occur at higher W for the neutron than for the proton.

3.8 Spin Dependent Nucleon Structure Functions

The proposed precision measurements of R will greatly aid the development of reliable global descriptions of existing inclusive electroproduction data on deuterium at moderate to high Q^2. This is critical for the extraction of the spin-dependent structure functions g_1 and g_2 from spin asymmetry measurements in the resonance region. The proposed measurements will allow a complete survey of the resonance region, and will permit an extraction of the Q^2 dependence of the L-T separated structure functions with very fine granularity in W^2 utilizing bins of (25 MeV)^2. Such models are necessary for accurate radiative correction calculations. Recently, both the CLAS [24] collaboration in Hall B and experiment E01-006 [25] in Hall C have completed electron spin asymmetry measurements utilizing ND3 targets. What was measured was the yield asymmetries for the scattering of beam electrons polarized both parallel and anti-parallel to the beam direction. For target polarizations both parallel and perpendicular to the beam direction, this yields the asymmetries $A_{||}$ and $A_{\perp}$, respectively. In Hall B it is possible to measure $A_{||}$ only, as perpendicular target fields are not feasible within the confines of the CLAS detector, while E01-006 was able to obtain both parallel and perpendicular target polarizations.

The photon helicity asymmetries, A_1 and A_2, can be determined from the electron asymmetries via

$$A_1 = \frac{C}{D}(A_{||} - dA_{\perp}), \tag{10}$$

and

$$A_2 = \frac{C}{D}(C^{'}A_{||} - d^{'}A_{\perp}). \tag{11}$$

The factors C, $C^{'}$, d, and $d^{'}$ are kinematic only, while the photon depolarization factor,

$$D = \frac{1 - \epsilon E^{'}/E)}{1 + \epsilon R}, \tag{12}$$

is a function of the unpolarized structure function ratio R. For $\epsilon R << 1$, the fractional uncertainty in $A_{1,2}$ coming from an uncertainty in R of δR is

$$\Delta A_{1,2}(\delta R) = \frac{\epsilon}{1 + \epsilon R} \approx \epsilon \delta R. \tag{13}$$

Using the World's previous proton average in the resonance region of $R = 0.06$ or a typical value from E94-110 of $R = 0.24$ leads to a difference of 9% in $A_{1,2}$ at $\epsilon = 0.5$.

It is important to note that it is a linear combination of A_1 and A_2 that appears as the integrand in the generalized Gerasimov-Drell-Hearn (GDH) integral [26, 27, 28]. The resonance region represents the largest contribution to this integral at small Q^2.

We would like to stress that both experiments measure electron scattering *asymmetries*, and therefore, require a parameterization of the unpolarized structure functions

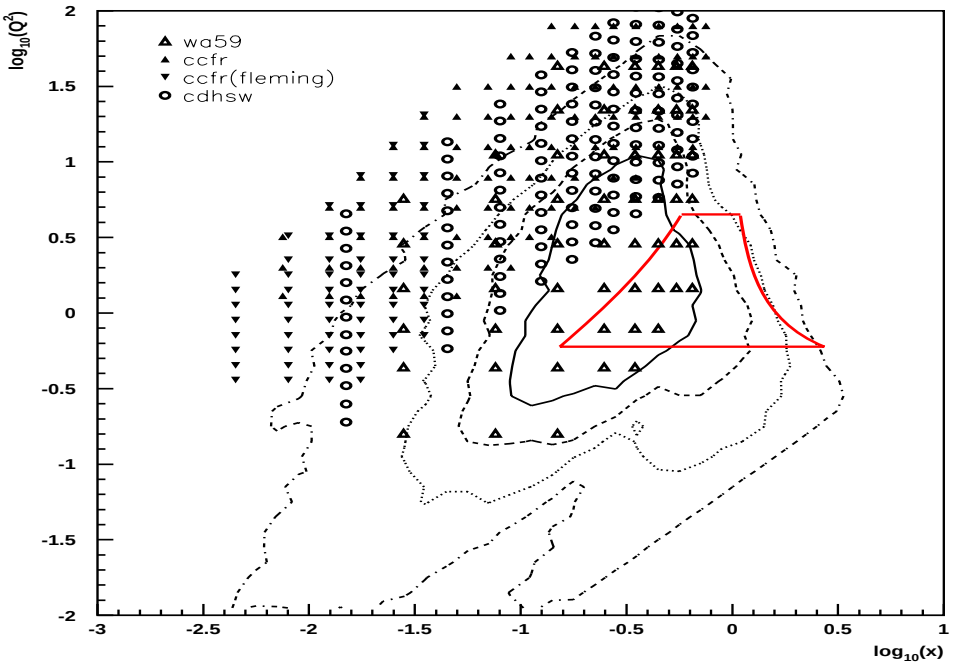

Figure 7: Kinematic coverage of the MINOS neutrino experiment at Fermilab. The data points indicate previous structure function measurements using neutrino beams and the red curve indicates the measurement region of this proposal.

in order to extract both $A_{1,2}$ and spin structure functions. For example, g_1 can be extracted via

$$g_1 = \frac{F_1(A_1 + \gamma A_2)}{(1+\gamma^2)} \propto F_1(1+\epsilon R) \propto \frac{F_2(1+\epsilon R)}{1+R}. \tag{14}$$

Therefore at $\epsilon \approx 1$ only knowledge of F_2 is needed for the extraction of g_1. It should be stressed that there has been no experiment in which the strength from F_2 and R have been separated for any significant portion of the resonance region. Hence, the relevant question becomes; how sensitive is the extraction of F_2 in the resonance region to different values of R?

3.9 Neutrino Cross Section Modeling

This section was taken verbatim from a letter written in support of this proposal by Hugh Gallager of Tufts University. We further note that neutrino physicists manned $\approx 1/3$ *of the shifts during the January 2005 run period. This large support from the neutrino community came from collaborators on many experiments, including K2K, JHF, mini-Boone, MINOS, and MINER*ν*A.*

Electron scattering data from deuterium in this kinematic regime will be of particular use to neutrino experimentalists. A current challenge for these experiments is how to

construct a cross section model in the resonance / DIS overlap region. Because high statistics neutrino data in this region is lacking, this model construction can have large uncertainties which in turn become important systematics.

Figure 7 shows the kinematic range probed by the MINOS experiment in its current energy configuration. Since the MINOS experiment uses two detectors, many model uncertainties cancel. A good understanding of the cross section in the 1-5 GeV range is nonetheless important, since it is in this energy range where the oscillation signal is expected to appear. Extracting precise values for the oscillation parameters from a near-far comparison in this energy regime relies on a good understanding of the underlying interaction physics [29].

The data points in Figure 7 indicate previous structure function measurements by neutrino experiments. The region indicated in red is that explored by this proposal. Neutrino measurements in this region have been very limited, the measurements from the WA59 CERN bubble chamber experiment, which overlap this proposal in kinematics, had combined uncertainties on F_2 in the range of 20 to 30%. In addition these measurements were from a neon target with the associated challenges of untangling nuclear effects.

While the data at lower Q^2 on nuclear targets is crucial for understanding nuclear effects, it is of less use than the data at higher Q^2 in the construction of a free nucleon cross section model. This is due to the fact that as $Q^2 \to 0$ the hadronic current is dominated by the axial component which is unexplored in electron scattering experiments. The kinematics of this proposal, on the other hand, provide a measurement of the vector current which contributes an equal amount to the neutrino cross section.

4 Measurement of the Inclusive Cross Section

The inclusive scattering cross section will be determined by measuring the yield of scattered electrons which will be detected in the High Momentum Spectrometer (HMS) in Hall C. Measurement of the inclusive cross section for a range of ϵ values at fixed W^2 and Q^2 requires that the beam energy be varied. For each beam energy, and with the spectrometer at a fixed scattering angle, the spectrometer momentum will be varied such that W^2 is scanned from the elastic kinematics out though the resonance region and into the DIS region to $W^2 \approx 4.0$ GeV^2. Performing such scans at a variety of beam energies and scattering angles allows the entire resonance region to be surveyed in a range of Q^2 and ϵ values for each small W^2 bin. Examples of four such scans performed during the January 2005 running are presented in Figure 8 as a function of W^2. The current bin width in W^2 is actually finer than that which will be used for the Rosenbluth separations of $\Delta W^2 \approx (25\ \text{MeV})^2$. The statistical errors bars are included, but are typically smaller than the symbol size.

Each plot includes up to 5 individual momentum settings with a momentum bite of $+/-8\%$ in the HMS spectrometer. Adjacent runs overlap in the momentum bite by $\approx 2\%$. This allows a good check on the spectrometer momentum acceptance. After applying acceptance corrections, the agreement between overlapping bins from adjacent runs is typically within the statistical uncertainties. The cross section in overlapping bins has been averaged in the plots presented here. Also plotted is the fit to previous JLab data [30] cross section data.

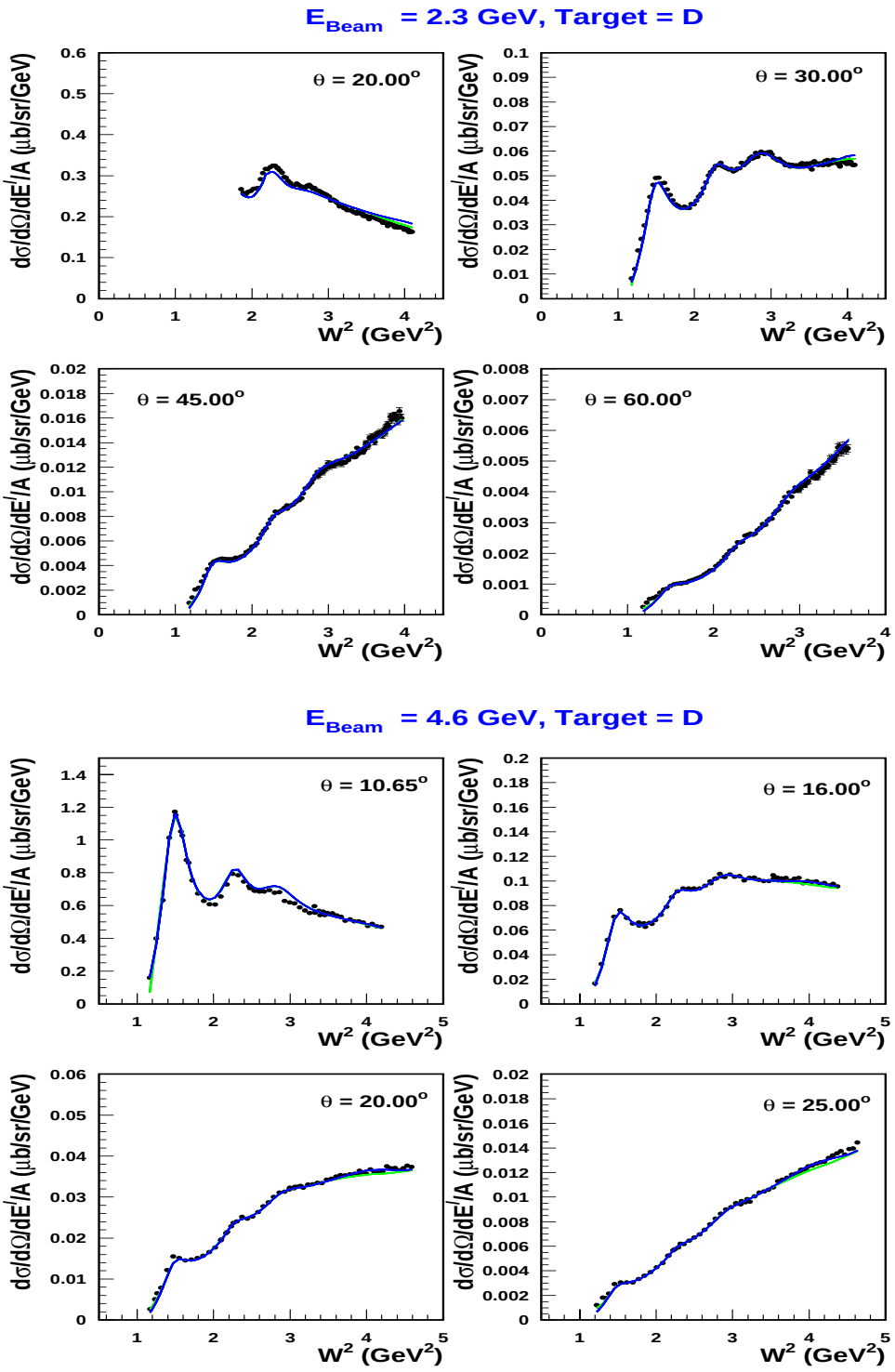

Figure 8: Preliminary low Q^2 inelastic deuterium cross sections measured in the January 2005 run period for beam energies of E = 2.3 GeV, and E = 4.6 GeV and for all spectrometer angle settings. The statistical errors are included, but are often smaller than the symbols. The blue (dark) curve is the model input to the radiative corrections.

5 Structure Function Extraction

The extraction of the structure functions from the cross section measurements will be accomplished in two complementary ways. First, Rosenbluth separations will be performed at each W^2, Q^2 where enough cross section measurements and range in ϵ exist to perform a good linear fit. Second, a global fitting procedure will be employed to separate the cross sections into longitudinal and transverse strength. Provided that enough of the kinematic space is covered, there is one unique way of doing this. Typical examples from the $\approx$ 200 Rosenbluth separations performed on the proton data is presented in Figure 9 at the various kinematics labeled on the plots. Since the individual cross section measurements were taken at slightly different Q^2, the fit to the data was used to move all ϵ points to a common Q^2. Care was taken that this movement was small enough so that the uncertainty introduced was much smaller than the experimental point-to-point uncertainties.

A subset of Rosenbluth separated R values extracted from the proton data in the range $1.5 < Q^2 < 2.5$ are presented in Figure 2 as a function of W^2 for the in Q^2. The same quality of data is expected for the proposed measurement and can be seen to be a vast improvement to the current World's data set when comparing to Figure 1. Interestingly, R exhibits resonance behavior heretofore only observed in F_2. This resonance structure can also be seen in F_1 and F_L, which were extracted from the proton Rosenbluth separations and are presented in Figure 6. Also plotted is the fit to the resonance cross sections, which is seen to be in excellent agreement with the Rosenbluth technique. A fit [7] of SLAC L-T separated DIS data is also shown and is seen to link smoothly to the resonance region data.

6 Systematic Uncertainties

At present, the world's best precision L-T separation measurements on deuterium have been performed by SLAC experiment E140X, to measure R in deep inelastic scattering. The point-to-point uncertainties for E140X are given in Table 3. The proposed experiment will be able to make resonance region measurements with a comparable level of precision. Much effort was put into both understanding and reducing the systematic uncertainties for E94-110. It is proposed that these same uncertainties will be achieved for this deuterium measurement. The point-to-point uncertainties for E94-110 are listed in Table 4. Also listed are the projected contributions to the cross section due to these uncertainties and the corresponding uncertainty in R extracted in the region of the Δ resonance.

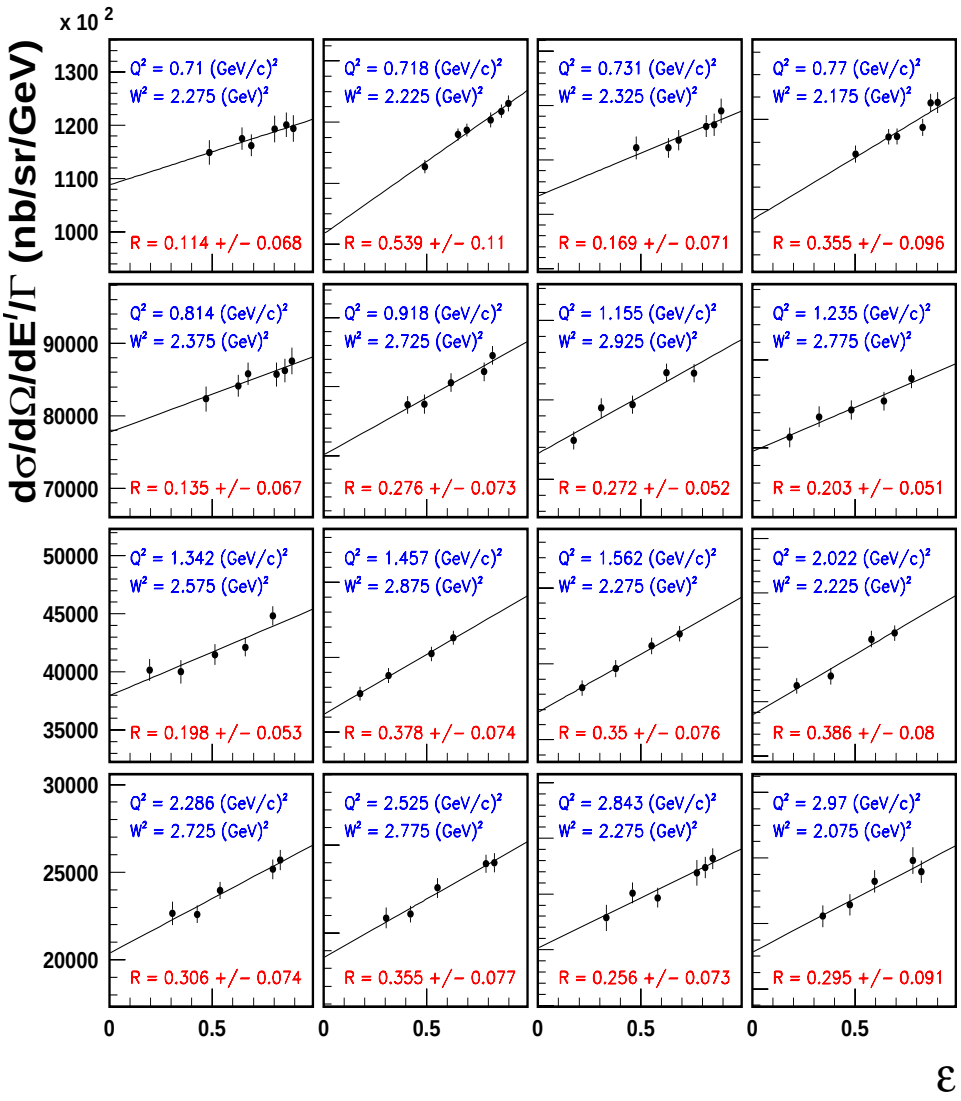

Figure 9: Typical examples of the ≈ 200 Rosenbluth separations performed on the E94-110 hydrogen data.

Experimental Quantity	Uncertainty	$\Delta\sigma(\%)$	ΔR
Beam Angle on Target	.05 mrad (.003^o)	0.1	0.005
Beam Energy	$1 \cdot 10^{-3}$	0.3	0.014
Scattered Electron Energy	0.05%	0.1	0.005
Target Density	0.2%	0.2	0.009
Scattering Angle	0.04 mrad (.002^o)	0.1	0.005
Beam Charge	$3 \cdot 10^{-3}$	0.3	0.014
Acceptance vs. θ	0.1%	0.1	0.005
Acceptance vs. p	0.1%	0.1	0.005
Detector Efficiency	0.1%	0.1	0.005
e^+/e^- background	0.1%	0.1	.005
Radiative Corrections	1.0%	1.0	0.000
	Total	1.1	0.039

Table 3: Published point-to-point systematic uncertainties from E140X.

Experimental Quantity	Uncertainty	$\Delta\sigma(\%)$	ΔR
		Δ ($Q^2 = 1.0$)	Δ
Beam Energy	$4 \cdot 10^{-4}$	0.3	0.011
Scattered Electron Energy	$4 \cdot 10^{-4}$	0.2	0.007
Target Density	0.01%	0.01	N/A
Scattering Angle	0.2 mrad	0.4	0.015
Beam Charge	$1 \cdot 10^{-3}$	0.1	0.004
Acceptance	0.6%	0.6	0.022
Detector Efficiency	0.4%	0.4	0.016
Deadtime Corrections	0.1%	0.1	0.004
e^+/e^- Background	0.2%	0.2	0.007
Radiative Corrections	1.0%	1.0	0.040
	Total	1.35	0.052

Table 4: Point-to-point systematic uncertainties from the analysis of E94-110 and the corresponding uncertainty on R for the region of the Δ resonance at $Q^2 = 1$ (GeV/c)^2.

6.1 Kinematics

One of the largest contributions to the point-to-point systematics comes from the uncertainties in the kinematics and is simply due to the large variation in the cross section with W^2 near the resonances. In order to help minimize these uncertainties, proton elastic scattering data will be taken at every beam energy and most HMS angle settings, where possible. For elastic scattering, the difference of the reconstructed invariant mass, W, from the proton mass ($\Delta W = W$ - M_p) can be constructed and the dependence of ΔW on possible energy and angle systematics can be studied.

Fitting the ΔW dependence on systematic energy and angle offsets allows an extraction of these offsets. This procedure was used for the E94-110 data and yielded an uncertainty in the corrected beam energy of 0.04% [31], less than half that typically quoted from Hall C Arc measurements. The reconstructed W values for these data are plotted verses scattering energy in Figure 6.1, for four different beam energies and twenty eight unique kinematic settings. It was found that the entire data set could be well described by assuming that the true HMS central angle was smaller than the nominal value by 0.5 mrad, and that the true HMS central energy was smaller than the nominal value by a constant fractional amount of -0.35%. The true beam energy was found to be smaller than the Arc measurements by an amount which varied with the energy. This was later confirmed by field mappings and corresponding calculations of the arc magnet field lengths, and typical Hall A and Hall C arc measurements now agree to better than 0.05%.

The reconstructed values for W are shown, both before (open symbols) and after (solid symbols) correcting for the kinematic offsets found from these studies. The corrected values are all seen to be within 1-2 MeV of the proton mass. We further note that the kinematic offsets from the E94-110 studies have been found to be consistent with a large number of subsequent Hall C experiments.

Accelerator cavity RF instabilities have been observed to cause variations in the beam energy on the order 0.05%. These variations of the beam energy can be measured using the BPMs (beam position monitors) in the Hall C Arc. These BPMs are read into the data stream every second and can be used to make relative beam energy corrections for the beam energy drift. Such corrections have been made by previous experiments and have resulted in the narrowing of missing mass peaks. Corrections for such beam energy variations were included in the proton analysis.

Just as the arc BPMs allow corrections for variations in beam energy to be made, information from the Hall C beamline BPMs allow corrections for beam position and angle on target to be made. In contrast to the arc BPMs, information from these BPMs are fed into the data stream on an event-by-event basis. Uncertainties in the beam position and angle on target directly translate into uncertainties in the reconstructed kinematics. We plan to use the Hall C uniform fast raster with a spot size on target of $\pm$ 1 mm. Deviations in the vertical position of the beam will appear as a momentum offset in spectrometers. The effect of a beam position offset can be calculated from the optical matrix elements for the spectrometer. The first-order forward matrix elements for the HMS spectrometer are given in Table 5. The effect on the reconstructed momentum due to a 1 mm offset of the beam on target in the spectrometer dispersive direction (x_{tar}) is

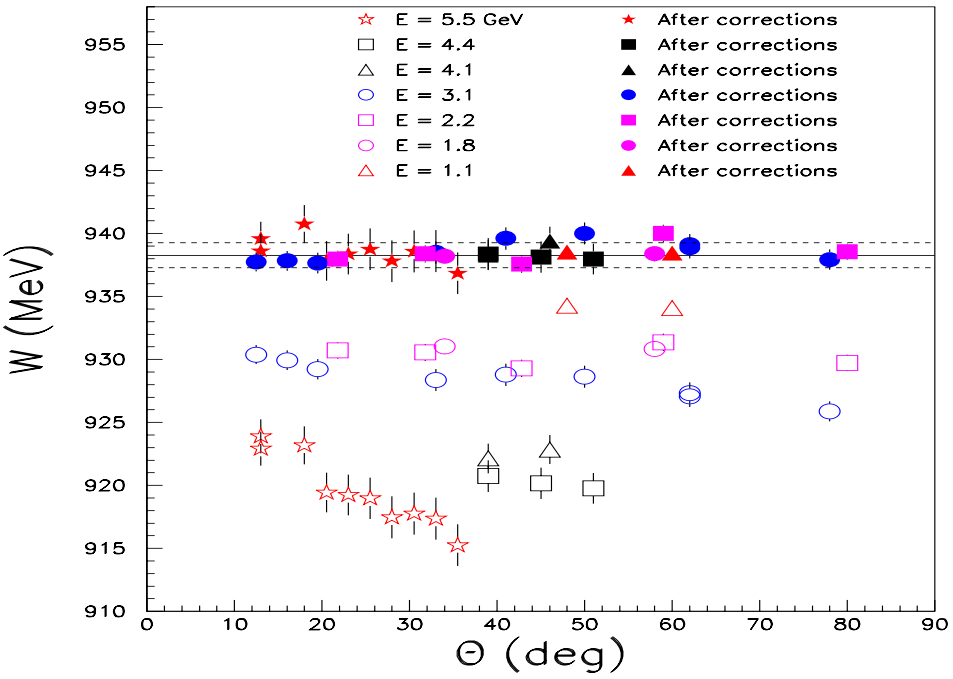

Figure 10: Reconstructed W vs. HMS momentum for elastic scattering kinematics. Open symbols represent data before kinematic corrections were applied, while the solid symbols represent the data after applying the kinematic corrections.

$$\Delta p(1\text{ mm}) = \pm 0.1\text{ cm} \cdot (-3.0821) \cdot 0.27\ (\%/\text{cm}) = \pm 0.08\%, \tag{15}$$

where the reverse matrix element (≈ 0.27 %/cm) has been used to convert $x^{'}_{fp}$ to δ.

A study of the run-to-run beam steering stability was made during the running of E94-110. From this study, we measure run-to-run variations in x_{tar} of $\delta x_{tar} < .2$ mm. We use this as a worst case, and calculate a corresponding point-to-point uncertainty in in spectrometer momentum, P, of

$$\Delta P = \pm 0.2 \cdot \Delta P(1\text{mm}) = .024\% \tag{16}$$

The angle of the beam on target ($x^{'}_{tar}$) enters as a direct uncertainty in the scattering angle if not corrected for. Again, the BPM information allows a correction to be made for this. The worst case point-to-point error is found to be the run-to-run $x^{'}_{tar}$ variations of $\Delta x^{'}_{tar} \approx .04$ mrad.

HMS	x_{fp}	x'_{fp}	y_{fp}	y'_{fp}
x_{tar}	-3.0821	0.05681	0	0
x'_{tar}	0.1555	-.3273	0	0
y_{tar}	0	0	-2.2456	-2.569
y'_{tar}	0	0	1.4135	-.2836
δ	3.7044	-0.001688	0	0

Table 5: HMS $1st$-order forward matrix elements.

6.2 Target Density

The disadvantage of using a small raster size is an increase in localized target density fluctuations. Localized target density fluctuations, induced by an intense incident beam, can significantly modify the average density of a cryogenic target. Point-to-point uncertainties in the target density and current enter directly as point-to-point uncertainties in the total cross section. The current-dependence can be measured by comparing the yields at fixed kinematics with varying beam currents. The deadtime-corrected yields should be proportional to the luminosity (and, therefore, the target density).

The result of such a 'luminosity scan' performed on the Hall C 'tuna can' deuterium target during Summer of 2003 is shown in Figure 11, where the charge normalized yield (N/Q) has been plotted versus the current. The N/Q ratios have been further normalized to ≈ 1 at a current of 20 μA. The error bars on the data are statistical only and do not reflect fluctuations in the beam current. The measured current dependence of the yield is 0.84 $\pm$0.29% per 100 μA. We note that the size of this correction has been significantly reduced with the introduction of the uniform square raster pattern.

Using the estimated error on the fit of $\pm$0.4% and a run-to-run variation in the current of ± 2 μA, the estimated point-to-point uncertainty in the target density is

$$\Delta\rho_t = 2\ \mu\text{A} \cdot \frac{0.4\%}{100\ \mu\text{A}} = 0.008\%. \tag{17}$$

We propose to use a constant beam current of 80 ± 2 μA for these measurements to reduce the uncertainty to this level.

Other quantities which contribute to a systematic uncertainty in the total cross section are corrections for acceptance, detector efficiencies, and deadtime. All of these have been studied for E94-110, E99-118, and a variety of other Hall C experiments and are believed to be well-understood. Reliable Monte Carlo models for both spectrometers exist, and have been shown to accurately reproduce the data for many different processes and kinematics. For the proton data, the model of the HMS was checked exhaustively and fine tuned to ensure the level of precision needed for high quality L-T separations.

6.3 Spectrometer Acceptance

A comparison of the HMS Monte Carlo to a typical proton run from January 2005 for kinematics near the delta resonance is shown in Figure 12. This includes comparisons

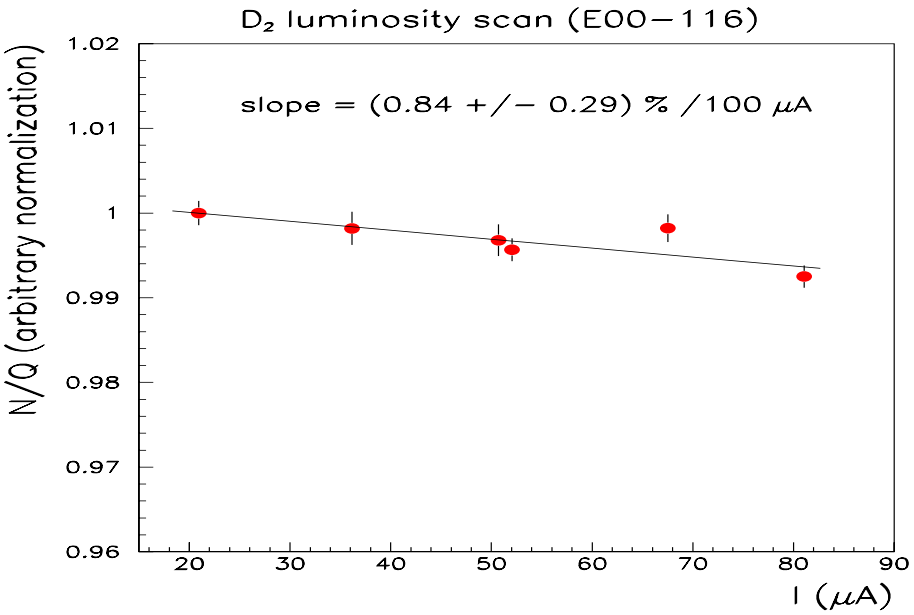

Figure 11: Cryogenic deuterium target luminosity scan from E00-116, utilizing the Hall C uniform raster. Plotted is the charge normalized yield (N/Q) versus beam current. The N/Q ratios have been further normalized to ≈ 1 at a current of 20 μA.

of the distributions for $\delta p/p$, $Y^{'}$ (the in-plane scattering angle), $X^{'}$ (the out-of-plane scattering angle), and $d\theta$ (the difference of the full scattering angle from the central spectrometer angle). Also shown is the ratio of data to Monte Carlo yields versus $d\theta$ and $\delta p/p$. The agreement is seen to be excellent. We note that the input model is the resonance region fit from **E94-110**, which typically reproduces the E94-110 cross sections to better than 3%. This agreement is representative of the reproduceablity of cross section measurements with the HMS in Hall C.

The point-to-point uncertainty in the acceptance corrections given in Table 4 has been estimated using this model of the HMS. For an extended target, there can be a relatively large difference in the acceptance for forward and backward angle scattering and is dominated by events being lost in the aperture defined by the second quadrapole magnet. Studies have been made of the effects on the acceptance due to shifts of various apertures within the uncertainty allowed by surveys of the spectrometer, as well as inaccuracies in the optics model. These studies indicate a combined point-to-point uncertainty on the acceptance and optics of about 0.6%.

6.4 Detector Efficiencies

The efficiencies for the HMS shower and Cerenkov counters have previously been studied for inelastic (e,e') scattering [30]. Since the efficiency of the shower counter calorimeter increases with scattered electron energy, our worst case for the present experiment is for the kinematics in which the scattering is at high W and Q^2, and, therefore, low momenta. The uncertainties in the efficiencies for this case are $\pm 0.2\%$ for both the shower counter and Cerenkov counter. Studies of the tracking efficiencies have shown that once the rate dependence has been corrected for, the run-to-run variations are largely dominated by statistics. For the statistics expected, this uncertainty is estimated at 0.3%. The overall

detector efficiency is estimated to be $\pm 0.4\%$

Proposed Kinematics

Table 6 lists the beam energies and angles where we propose to measure the deuterium cross section. The kinematics have been chosen to maximize the number of L/T separation and the $\Delta\epsilon$ ranges. The latter is important for reducing the systematic uncertainty on the separated cross sections. The low Q^2 kinematics measured in January 2005 is shown in the top panel Figure 6.4, while the proposed measurements are included in the bottom panel. Small ranges in W^2 and Q^2 with measurements at different beam energies (different ϵ) are where L/T separations can be performed.

For each angle the HMS central momentum can be varied to scan from the quasielastic through the resonance region utilizing a momentum bite of $\pm 8\%$ (with 1% overlap for runs at adjacent momenta). The HMS central angle can be changed by 10 degrees in several minutes and studies indicate that the random angle uncertainty incurred is better than 0.2 mrad. On the other hand, changing the HMS central momentum requires 20 minutes or more for the magnets to stabilize. To minimize the overhead needed for kinematic changes we plan to scan through all the relevant HMS angles at fixed momentum and then change the HMS central momentum and rescan in angle, in order to cover all the kinematics required for each beam energy.

The differential cross sections for inclusive electron scattering will be measured according to the following definition:

$$\frac{d^2\sigma}{d\Omega dW^2} = \frac{\Delta N}{\Delta\Omega\Delta W^2}\frac{1}{Qnd}, \tag{18}$$

where ΔN is the counts per W^2 bin, n is the density of deuterium, d the target thickness, and Q is the integrated number of incident electrons on target. A minimum time of one quarter hour per kinematic setting and a beam current of 80 μA (40 μA for Aluminum) has been assumed. The time requirements listed are the estimated data acquisition times for the entire momentum scan at fixed angle, assuming an effective solid angle for the HMS of 6.5 mSr, and was determined such that the statistical accuracy per W^2 bin was ≈ 2 times better than the systematic point-to-point accuracy expected. The rates were estimated based upon a fit of previous deuterium resonance region cross section data from JLAB [30]. The SOS will be used to collect positron yields (predominantly from neutral pion production) for charge symmetric background studies and will be run in a simultaneous single arm mode with the HMS data, such that this adds little to the beam time request.

The extraction of neutron structure functions requires the subtraction of the proton data taken in E94-110 (after accounting for Fermi motion, binding, and off-shell effects). As a cross check on relative normalizations, we propose to do measurements of the hydrogen resonance region cross sections for $Q^2 < 3$ GeV^2 to compare to E94-110. This will require an additional 16 hrs. A minimum central spectrometer momentum setting of 400 MeV/c was assumed. All proposed measurements will use the Hall C 4 cm deuterium target. In addition, elastic proton data will be taken for a portion of the angle settings for kinematic checks.

The chosen beam energies in the table assume a linac energy of 1.14 GeV (2.35, 3.49, 4.63, and 5.77 GeV), with the exception of the beam energy, E = 4.05, which assumes a linac energy of 0.80 GeV (4.05 GeV). Both base energies are standard CEBAF accelerator tunes.

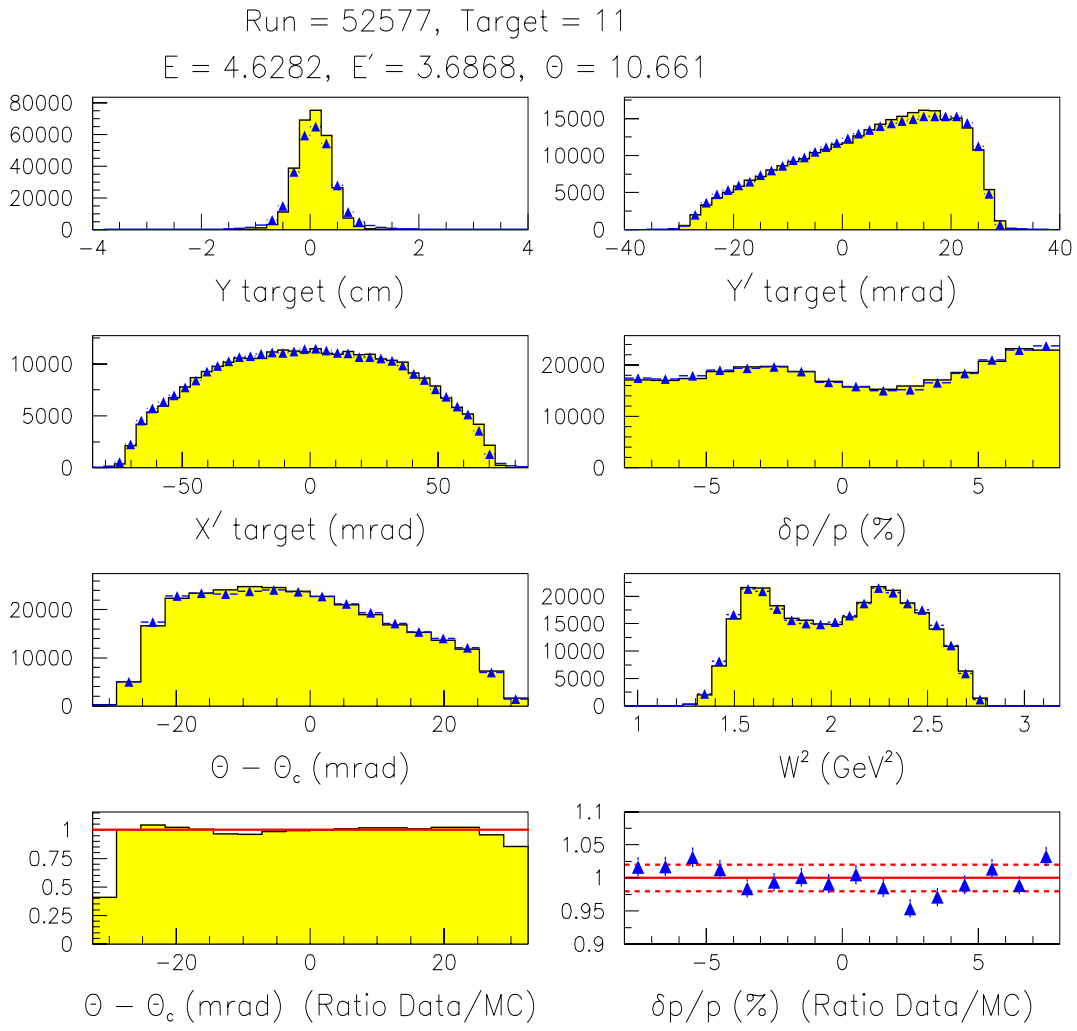

Figure 12: Comparison of hydrogen data taken during January 2005 (blue triangles with error bars) to the HMS Monte Carlo (yellow histograms) for the reconstructed vertex quantities which are described in the text. The input cross section model for the MC was the fit to the E94-110 data.

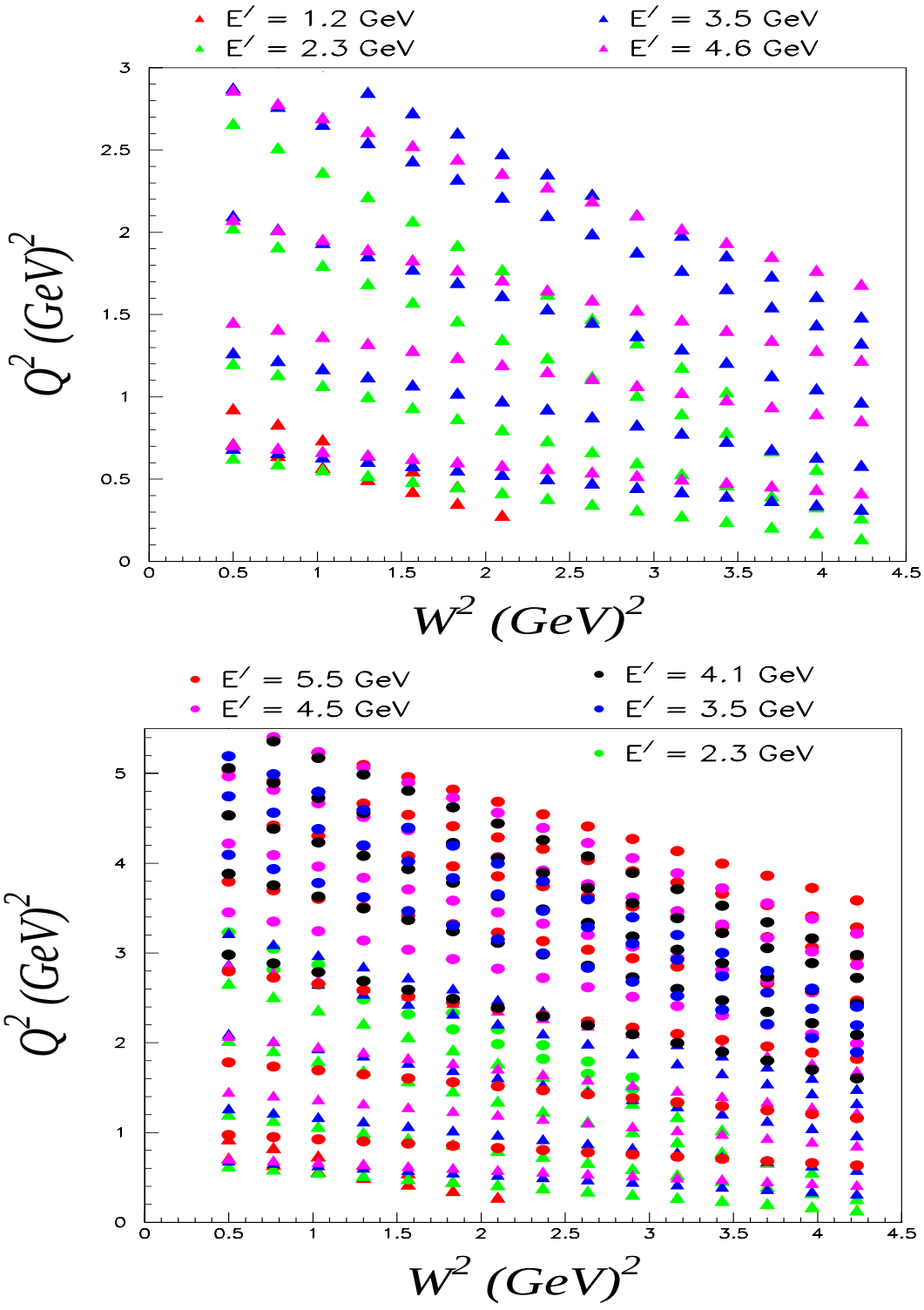

Figure 13: Kinematic covering of the low Q^2 run period of January of 2005 (top panel) and including the proposed measurements (bottom panel) which will both extend the L/T separations to higher Q^2 and add additional ϵ measurements at lower Q^2 to further reduce the uncertainties on the separated structure functions.

E (GeV)	θ (deg)	Q^2_Δ (GeV^2)	ϵ_Δ	Q^2_3 (GeV^2)	ϵ_3	Time for scan (Hours)
2.35	70	2.4	0.31	1.5	0.21	6
	80	2.5	0.24	1.6	0.16	10
3.49	52	3.5	0.44	2.7	0.35	10
	65	4.0	0.30	3.1	0.23	22
	78	4.4	0.20	3.4	0.15	35
4.63	30*	3.2	0.76	2.7	0.69	2
	36*	3.9	0.65	3.2	0.58	4
	43	4.6	0.54	3.8	0.47	6
	50	5.0	0.46	4.3	0.38	16
5.77	10.6	1.0	0.98	0.8	0.95	1
	15	1.8	0.95	1.5	0.90	1
	20	2.8	0.89	2.4	0.84	1
	25*	3.7	0.82	3.2	0.76	2
	29*	4.4	0.76	3.8	0.69	2
	32*	4.9	0.71	4.2	0.64	4
	35*	5.4	0.65	4.6	0.59	5
4.05	30*	2.5	0.75	2.0	0.67	2
	38*	3.3	0.63	2.7	0.54	2
	45	3.9	0.53	3.1	0.45	6
	52	4.4	0.44	3.5	0.37	11
	60	4.8	0.35	3.8	0.30	23
						Total **171**

Table 6: Beam time requirements for the proposed deuterium measurements. The time listed is that required to scan from the quasielastic to $W^2 \approx 4.5$ GeV^2. Positron data will be taken in the HMS for the angles indicated by an asterisk.

The beam time requested for this experiment is listed in Table 7. The total data acquisition time listed reflects the total time from Table 6 needed to complete the measurements on deuterium. We also require 35 hours for dummy target runs ($\approx 20\%$ of the deuterium time) which are needed to subtract the yield contributions from the aluminum end caps of the target, 16 hours to complete the hydrogen elastic scattering measurements, and 16 hours to obtain the hydrogen resonance region data which will be used to cross check with E94-110. Also, since the SOS spectrometer has a maximum central momentum of 1.75 GeV, we request an additional 22 hours to complete positron measurements in the HMS for larger scattering momenta at the angles denoted by an asterisk in Table 6. We assume 5 minutes for each angle change required at a given beam energy, and one-third hour for each spectrometer central momentum changes. Combined with 2 shifts for checkout, we request a total beam time of 13 days.

	Time Required (Hours)
Data acquisition (Deuterium)	171
Data acquisition (Dummy)	35
Data acquisition (hydrogen elastics)	16
Data acquisition (hydrogen resonance region)	16
Data acquisition (additional positrons)	22
Spectrometer momentum changes (35)	12
Angle changes (≈ 140)	12
Major beam energy changes (1)	8
Minor beam energy changes (3)	12
Checkout	16
Total	**320**

Table 7: Breakdown and tabulation of the total time requested. Based on previous experience, we assume 5 minutes for angle changes, 20 minutes for momentum changes, 8 hours for linac energy changes (major), and 4 hours for each energy change accomplished by changing the number of cycles (minor).

The Collaboration

The collaboration consists of people who have participated in a substantial amount of Hall C running. The collaboration has implemented and proven successful techniques to reduce systematic uncertainties in Hall C experiments, including detailed studies of spectrometer optics, spectrometer survey studies, raster phase analysis, and additional beam line instrumentation. This collaboration has the on-site experience, knowledge and expertise requisite to perform a precision measurement of the type proposed.

Summary

Using the Hall C base equipment, we propose to perform a global survey of L/T separated unpolarized structure functions on deuterium throughout the nucleon resonance region with an order of magnitude better precision than has been achieved before. In particular, the Q^2 and W^2 dependence of the separated structure functions will be measured for the first time. The recent analysis of the proton data from E94-110 clearly show that these goals are both realistic and attainable. We request 13 days to perform these fundemental measurements.

REFERENCES

1. JLAB experiment 02-109, M.E. Christy and C.E. Keppel spokespersons.
2. JLAB experiment 94-110, C.E. Keppel spokesperson.
3. E94-110 Collaboration (Y. Liang, *et al.*), nucl-ex/0410027.
4. JLAB experiment 99-118, A. Bruell, J. Dunne, and C.E. Keppel spokespersons.
5. V. Tvaskis, Ph.D. Thesis, Vrije Universiteit (2004).
6. M.N. Rosenbluth, Phys. Rev. 79, 615 (1956).
7. L.W. Whitlow *et al.*, Phys. Lett. B250, 193 (1990).
8. S. Dasu *et al.*, Phys. Rev. Lett. 61, 1061 (1988).
9. L.H. Tao, Ph.D. Thesis, The American University (1994).
10. BCDMS Collaboration (A.C. Benvenuti *et.al*), Phys.Lett. B237, 592 (1990).
11. M. Ericson and S. Kumano, Phys. Rev. C **67**, 022201 (2003), [arXiv:hep-ph/0212001].
12. JLAB experiment E03-012 (BoNuS), S. Kuhn, C.E. Keppel, and W. Melnitchouk spokespersons .
13. D. Dolgov, *et al.*, Phys. Rev. D66 (2002).
14. QCDSF Collaboration (M. Gockeler *et al.*) , hep-ph/0410187.
15. W. Detmold, W. Melnitchouk, and A.W. Thomas, Phys. Rev. D66, 54501 (2002).
16. A. Lung, *et al.*, Phys.Rev.Lett.70, 718(1993).
17. W. Melnitchouk, R. Ent, and C. Keppel, Phys.Rept.406, 127 (2005).
18. Phys. Rev. D64, 054004 (2001).
19. W. Melnitchouk,Nucl. Phys. A699, 278 (2002).
20. P. Eden *et al.* JHEP110 40,2001.
21. S. Jeschonnek, hep-ph/0201113.
22. S. Liuti, hep-ph/0111063.
23. F.E. Close and N. Isgur, Phys.Lett. B509, 81 (2001).
24. JLAB experiment E93-009, S.E. Kuhn spokesperson.
25. JLAB experiment E01-006, O. Rondan spokesperson.
26. S.B. Gerasimov, Sov. J. Nucl. Phys. 2, 430 (1966).
27. S.D. Drell and A. C. Hearn,Phys. Rev. Lett. 16,908 (1966).

28. X. Ji, C. Kao and J. Osborne, Phys. Lett. B 472, 1 (2000).

29. MINERvA Collaboration (D.A. Harris *et al.*), FERMILAB-PUB-04-252-E, JLAB-PHY-04-52, Oct 2004, e-Print Archive: hep-ex/0410005

30. I. Niculescu. Ph.D. Thesis, Hampton University (1999).

31. E94-110 Collaboration (M.E. Christy *et al.*), Phys.Rev.C70:015206 (2004)

32. I. Niculescu, J. Arrington, R. Ent, and C.E. Keppel, hep-ph/0509241 (submitted to Phys. Rev. C).

Appendix A: DOE Milestones for Hadronic Physics

Year	**Milestones:**
2008	Make measurements of spin carried by the glue in the proton with polarized proton-proton collisions at center of mass energy, $\sqrt{s_{NN}} = 200$ GeV.
2008	Extract accurate information on generalized parton distributions for parton momentum fractions, x, of 0.1 - 0.4 , and squared momentum change, –t, less than 0.5 GeV^2 in measurements of deeply virtual Compton scattering.
2009	Complete the combined analysis of available data on single π, η, and K photo-production of nucleon resonances and incorporate the analysis of two-pion final states into the coupled-channel analysis of resonances.
2010	Determine the four electromagnetic form factors of the nucleons to a momentum-transfer squared, Q^2, of 3.5 GeV^2 and separate the electroweak form factors into contributions from the u, d and s-quarks for $Q^2 < 1$ GeV^2.
2010	Characterize high-momentum components induced by correlations in the few-body nuclear wave functions via (e,e'N) and (e,e'NN) knock-out processes in nuclei and compare free proton and bound proton properties via measurement of polarization transfer in the $^4He(\vec{e},e'\vec{p})^3H$ reaction.
2011	Measure the lowest moments of the unpolarized nucleon structure functions (both longitudinal and transverse) to 4 GeV^2 for the proton, and the neutron, and the deep inelastic scattering polarized structure functions $g_1(x, Q^2)$ and $g_2(x,Q^2)$ for x=0.2-0.6, and $1 < Q^2 < 5$ GeV^2 for both protons and neutrons.
2012	Measure the electromagnetic excitations of low-lying baryon states (<2 GeV) and their transition form factors over the range $Q^2 = 0.1 – 7$ GeV^2 and measure the electro- and photo-production of final states with one and two pseudoscalar mesons.
2013	Measure flavor-identified q and $\bar{q}$ contributions to the spin of the proton via the longitudinal-spin asymmetry of W production.
2014	Perform lattice calculations in full QCD of nucleon form factors, low moments of nucleon structure functions and low moments of generalized parton distributions including flavor and spin dependence.
2014	Carry out ab initio microscopic studies of the structure and dynamics of light nuclei based on two-nucleon and many-nucleon forces and lattice QCD calculations of hadron interaction mechanisms relevant to the origin of the nucleon-nucleon interaction.

Figure 14: